ACS OMEGA

http://pubs.acs.org/journal/acsodf

Article

Exceeding the Boundaries of the Paraxial Spatiotemporal Nonlinear Optics and Filamentation for Ultrashort Laser Pulses

Ekaterina Iordanova,* Georgi Yankov, Stefan Karatodorov, and Lubomir Kovachev

Cite This: *ACS Omega* 2023, 8, 3501−3508

Read Online

ACCESS | Metrics & More | Article Recommendations

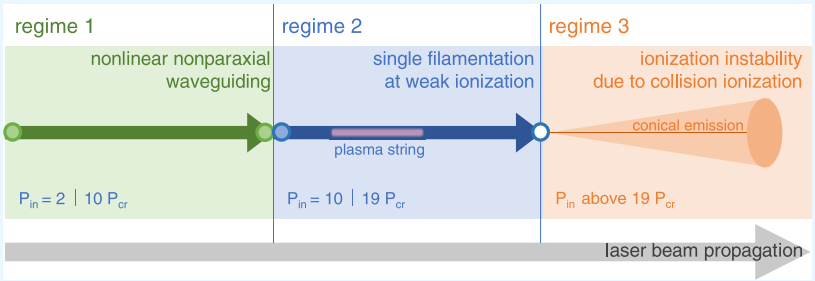

ABSTRACT: An impressive phenomenon of observed plasma instability and conical emission under the propagation of ultrashort laser pulses in the air is reported. The discussed novel findings demonstrating nonlinear effects are incapable to be explained in the standard spatiotemporal paraxial optics. Three main mechanisms are investigated. The first one is related to the nonlinear nonparaxial mechanisms for waveguiding of femtosecond pulses, and the second one considers the mechanism of single filament formation at weak ionization. The third mechanism demonstrates a new physical effect leading to collision ionization with intensities in the range of 10^{10}−10^{11} W/cm^2. Furthermore, a new ionization regime of instability is suggested at intensities below the critical thresholds for multiphoton and tunnel ionization. The experimental results and findings are supported by theoretical analyses and numerical simulations.

1. INTRODUCTION

The progress of laser technology in the last three decades has allowed for the generation of ultrashort laser pulses with powers up to a few petawatts. This extraordinary achievement became possible with the development of the chirped pulse amplification technique for amplifying an ultrashort (femtosecond) laser pulse.[1] Naturally, the new technology horizon permitted observation of novel nonlinear optical phenomena such as filamentation,[2−4] conical emission,[5−7] coherent GHz-emission in the air,[8,9] rotation of the polarization plane,[10] merging and energy exchange between filaments,[11−14] and so forth. Consequently, a new filamentation regime for the propagation of powerful femtosecond laser pulses in the air is reported, for the first time, by Braun et al.[2] In its origin, the filamentation process is characterized by waveguide propagation with power above the critical for self-focusing, a supercontinuum (white) spectra, and the observation of plasma channels in the laser beam spot. Thereby, the initial explanation of the filamentation genesis started with the nonlinear process of self-focusing of the femtosecond laser pulse. The field intensity in the filament core achieved values in the range of 10^{13}−10^{14} W/cm^2, which became high enough for plasma generation. Hence, the self-focusing effect is demolished by the plasma defocusing. Therefore, it is proposed that the periodic process of self-focusing and plasma defocusing initiate the start of a waveguide propagation regime. The first theoretical models of filamentation are focused on this balance between self-focusing and plasma-defocusing.[3,4] Several years later, this is reported for laser pulse filamentation formation in the waveguiding regime, without plasma generation.[15−17] The field intensity of the stable filament in the experiments is reported to be in the order of 10^{10}−10^{11} W/cm^2 and insufficient for plasma generation. In a recent work,[18] in an experimental investigation with 35 fs pulses, we demonstrated a new waveguiding regime with powers up to 10 times higher than the critical one for self-focusing. In this work, we report on another impressive phenomenon, a plasma instability and conical emission under investigation with ultrashort 35 femtosecond laser pulses. The discussed novel findings of the authors related to the observed new nonlinear effects are impossible to be explained in the frame of the well-known spatial−temporal paraxial optics.

Received: December 2, 2022
Accepted: December 28, 2022
Published: January 11, 2023

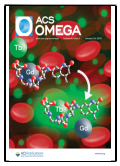

https://doi.org/10.1021/acsomega.2c07703
ACS Omega 2023, 8, 3501−3508

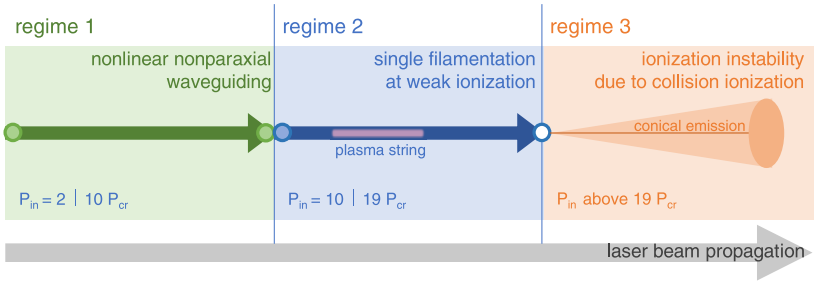

Figure 1. Schematic view of the three investigated regimes of laser beam propagation as a function of the laser power P_{in} to the critical power for self-focusing P_{cr}. Regime 1 corresponds to nonlinear waveguiding with an absence of plasma. Regime 2 corresponds to single filamentation, with a very weak plasma string. Regime 3 represents a strong plasma string along with the propagation distance and conical emission.

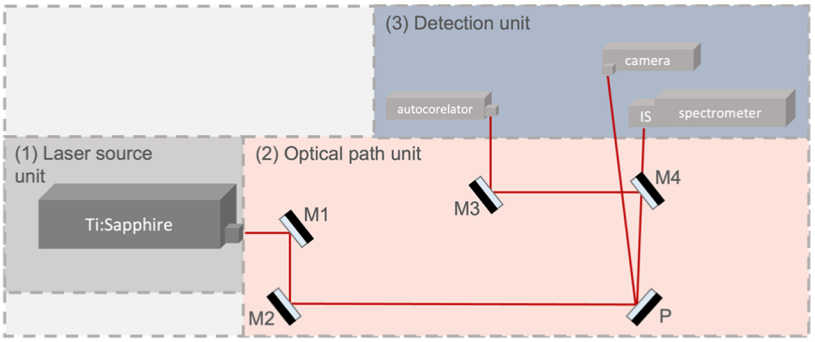

Figure 2. Schematic view of the setup configuration consisting of (1) laser source unit—Ti: Sapphire femtosecond laser system with a repetition rate of 1 kHz and emitting at an 800 nm central wavelength with a pulse duration of 35 fs; (2) optical path unit—guiding the laser beam path at a distance of 80 m using M1 ÷ M4 low GDD ultrafast mirrors and a 2° round wedge prism P; and (3) detection unit—laser beam profiler, high-resolution spectrometer, autocorrelator, and integrated sphere (IS).

Moreover, a new ionization regime of instability is performed at intensities below the critical thresholds for multiphoton and tunnel ionization. Subsequently, in this paper three main directions of the experimental and theoretical approach to ensure coherence and consistency of the investigation are considered. The three investigational directions (see Figure 1) are as follows: (1) investigating the nonlinear nonparaxial mechanisms for waveguiding of fs pulses, (2) investigating the single filament with weak ionization, and (3) investigating the mechanism of a new physical effect leading to collision ionization and conical emission with intensities in the range of 10^{10}–10^{11} W/cm^2, which is significantly below the critical thresholds for multiphoton and tunnel ionization. Schematically, the three main regimes describing the laser beam propagation and the above-considered directions are illustrated in Figure 1.

Generally, depending on the incident polarization, linear, elliptic, or circular, the nonlinear polarization is of the Marker and Terhune type. This type of polarization in the case of gas media produces self-phase modulation (Kerr type) nonlinearity, cross-phase modulation, and degenerate four-photon parametric mixing. In the cases where only the amplitude A_x linearly polarized component exists, the Marker and Terhune nonlinear polarization is transformed to typical Kerr-type nonlinearity only. Because of this, in the current research, where the laser system provides linear polarization of the beam, a scalar Kerr-type nonlinearity for the A_x component of the electrical field is applied. Further, the scalar nonlinear nonparaxial equation governing the pulse propagation is solved.

Our starting point in regime 1 is the nonlinear nonparaxial amplitude equation (NNAE), which describes the nonparaxial optics of laser pulses

$$2ik_0\left[\frac{\partial A}{\partial z}+\frac{1}{v_{gr}}\frac{\partial A}{\partial t}\right] = \Delta_\perp A+\frac{\partial^2 A}{\partial z^2}-\left(\frac{1+\beta}{v_{gr}}\right)\frac{\partial^2 A}{\partial t^2}+k_0^2 n_2|A|^2 A \quad (1)$$

Further norming it in Galilean frame $z_1 = (z - V_{gr}\cdot t)/Z_0$; $t_1 = t/t_0$; and $A(x,y,z,t) = A_0A(x,y,z,t)$ and considering that under investigation, we have $\alpha = k_0z_0$; $\delta^2 = d_0^2/z_0^2$; and $\beta = z_{dif}/z_{dis}$; $\gamma = 1/2k_0^2d_0^2n_2|A_0|^2$ one can get the equation governing the pulse evolution in media without group velocity dispersion in the following form

$$2i\alpha\delta^2\frac{\partial A}{\partial t_1} = \Delta_\perp A-\delta^2\left(\frac{\partial^2 A}{\partial t_1^2}-2\frac{\partial^2 A}{\partial t_1\partial z_1}\right)+\gamma|A|^2A \quad (2)$$

Linear terms; Nonparaxial terms; Nonlinear term

where the different terms are indicated in a circled manner, $\Delta_\perp$ is denoted as the transverse Laplacian, and k_0 is the linear wavenumber. The variable A is the amplitude envelope of the optical pulse ($A = A_x$ is the x component of the amplitude envelope and $A_y = 0$). The group velocity is denoted as v_{gr}. The dispersion length is given by $z_{dis} = t_0^2/k''$, where t_0 is the time duration of the pulse, and k'' is the group velocity dispersion. The diffraction length, $z_{dif} = k_0d_0^2$, where d_0 is the spot radius at level e^{-1} from the amplitude maximum. The longitudinal spatial size of the pulse is $z_0 = v_{gr} \times t_0$. The nonlinear refracted index is signed by n_2. The constants α and δ^2 and are applied

https://doi.org/10.1021/acsomega.2c07703
ACS Omega 2023, 8, 3501−3508

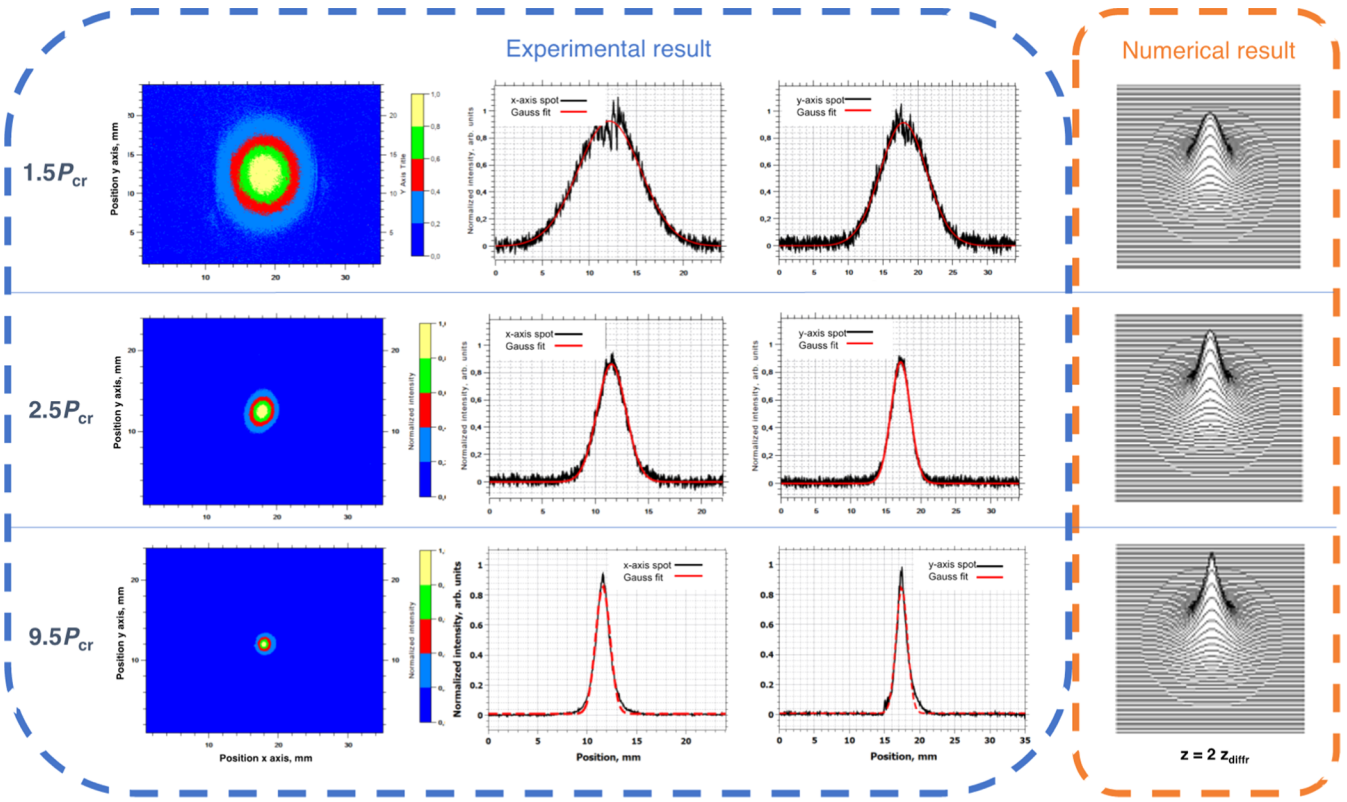

Figure 3. Experimental and numerical results at three initial laser powers P_{in} equal to 1.5P_{cr}, 2.5P_{cr}, and 9.5P_{cr}. A part of the experimental result showsk in each row images of the laser spot and its distribution in *x*- and *y*-direction with Gaussian fit in the red line. The numerical results on the right side show similar spot distribution and confirm the experimental results of waveguiding and weak self-focusing under the investigated conditions.

with values, which correspond exactly to the experimental conditions (at an 800 nm central wavelength, a pulse duration of t_0 = 35 fs, and a spot radius of d_0 = 0.4 cm). The dispersion length at 35 fs pulse is still larger than the diffraction lengths, and the dispersion number is small enough ($\beta = z_{dif}/z_{dis} < 1$) and is neglected in the following analysis. In the case of the dimensionless form, in addition to the well-known numbers α and δ^2, a new nonlinear wavenumber appears $\gamma = k_0^2 d_0^2 n_2 |A_0|^2 = z_{dif}/z_{nl}$, where $z_{nl} = 1/k_0 n_2 |A_0|^2$ is the nonlinear length. In regime 2, experimentally is observed a weak plasma string, which does not affect the waveguide propagation, and the effect of the plasma in regime 2 is neglected. To further describe regime 3 introduction of the conical emission is considered for plasma generation all over the laser propagation by proposing a new type of collision ionization regime based on the confinement of an ensemble of neutral particles into pulse envelopes and collision with the free particles. The trapped particles are translated with a group velocity and admit kinetic energy that is enough to ionize by colliding with the free particles on the way. The focus of this work is on the three regimes further described in the paper as follows: (1) nonlinear nonparaxial waveguiding regimes, (2) single filamentation with weak ionization, and (3) ionization instability due to collision ionization.

2. EXPERIMENTAL SETUP CONFIGURATION

The schematic representation of the experimental setup is outlined in Figure 2. The setup configuration consists of three main units—a laser source, an optical path, and a detection unit. The laser source unit: (1) the laser pulse is generated by a femtosecond (fs) laser system (Spectra-Physics, Spitfire Ace). The regenerative Ti: Sapphire amplifier emits at a central wavelength of 800 nm, with a pulse duration of 35 fs, and operates at a 1 kHz repetition rate. The optical path unit: (2) the laser beam is guided via four (M1÷ M4) low GDD ultrafast mirrors and one 2° round wedge prism P to the detection systems.

The error margins regarding the positioning of the optical and optomechanical elements are estimated to be in the range of ±0.4−1 mm. The total optical path of the beam under investigation is 80 m, and the distance between mirror M2 and the wedge prism P is 70 m. To avoid any doubts that the observed effects are only due to air nonlinearities, it used an initial linearly polarized laser pulse, and all optical elements are removed from the optical path of the laser beam, except the two M1 and M2 ultrafast plane mirrors to guide the beam to a long distance (mirrors M3 and M4 are at a distance of a few cm from the observation equipment). The detection unit: (3) the equipment used for detection and analyses of the laser beam includes a laser beam profiler (Spiricon, Ophyr), an autocorrelation system (GRENOUILLE 8-20-USB), a high-resolution spectrometer (Ocean Insight HR4000), and an integrated sphere (Thorlabs). The experimental setup is further equipped with a power meter (Ophyr, Nova II) and optical and optomechanical components. The autocorrelation system is applied to monitor and control the main output parameters of the fs laser radiation. The laser beam profile and the variations in the laser beam size are analyzed and visualized via a beam profiler. The spectra are performed by a spectrometer system consisting of an integrated sphere,

https://doi.org/10.1021/acsomega.2c07703
ACS Omega 2023, 8, 3501−3508

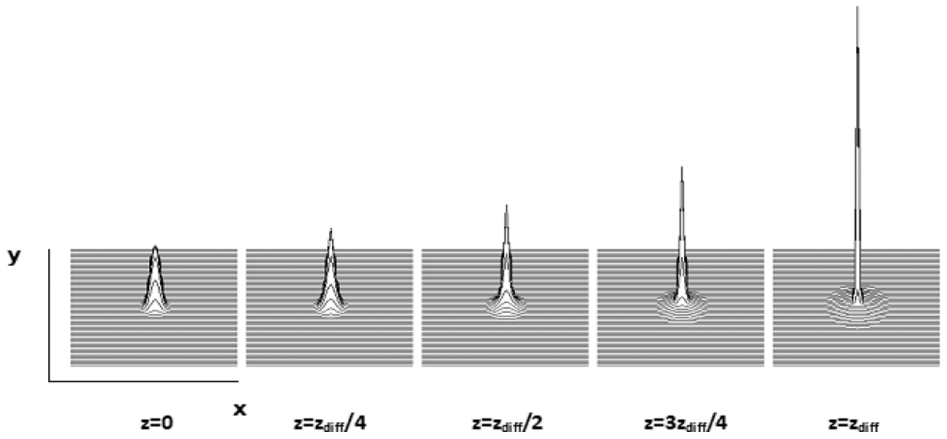

Figure 4. Self-focusing of a nanosecond Gaussian optical pulse with initial power $P_{in} = 3P_{cr}$, obtained from numerical simulation with STNE (3). Projection the spot intensity $|A(x,y)|^2$ for different distances from the source, in units of diffraction lengths. The nonlinear focus on a broad pedestal is formed at one diffraction length.

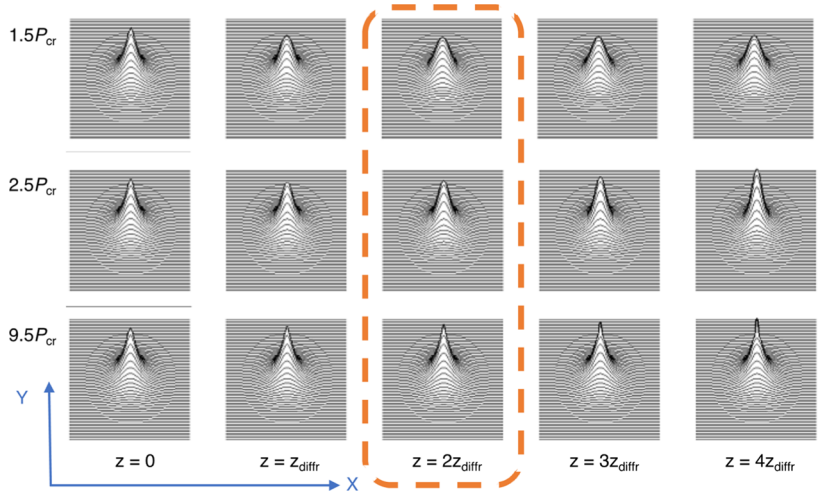

Figure 5. Numerical simulation results of the evolution of the laser pulse at different diffraction lengths governed by NNAE (2). The case at a distance corresponding to two diffraction lengths is compared with experimental results in Figure 3.

collecting the beam signal, and a high-resolution spectrometer. Performing the experiments with the different regimes, the beam is either kept or split into two parts before the detection unit via the wedge prism. The flip-flop option of mirror M4 allows the beam signal to be measured with the autocorrelator and the spectrometer. To guide the laser beam over a long distance, only planar mirrors are used to avoid any possibility of focusing and phase deformation. This condition ensures that all effects due to the diffraction of the 35 femtosecond pulse propagation are obtained from the propagation in air. Furthermore, it is important to note that when the optical response of the electronic nonlinearity is in the order of 2.5 fs (2.5×10^{-15} s), the atoms and molecules are polarized and then emit at the same frequency. In the performed experiments, at a repetition rate of 1 kHz, the time distance between the pulses is 1 ms (1×10^{-3} s) and for this period of a millisecond, the medium is relaxed to its basic state, and no thermal effects can be expected.

3. RESULTS AND DISCUSSIONS

3.1. Nonlinear Nonparaxial Waveguiding Regime. *3.1.1. Experimental Investigation.* The critical power for self-focusing is $P_{cr} = \lambda_0(0.61)2\lambda_0 2/8n_0n_2$, where n_0 is the refractive index in air ~1, and the nonlinear refractive index n_2 is equal to 5×10^{-19} cm/W^2. At the central wavelength of the laser, at λ_0 = 800 nm, the estimated value for the critical power for self-focusing on air is found to be $P_{cr}^{air} = 1.8 \times 109$ W. The power range describing this regime for the laser power P_{in} is $1.5P_{cr} < P_{in} < 10P_{cr}$, where P_{cr} is the power for self-focusing. A characteristic feature of this waveguided propagation is that the transverse Gaussian profile of the pulses up to $P_{in} = 9.5P_{cr}$ is preserved. The experimentally applied laser pulse power P_{in} is varied in the range of 80−600 μJ. The values are obtained as follows: (i) at a laser power of 80 μJ, the $P_{in} = 1.5P_{cr}$; (ii) at a laser power of 160 μJ, the $P_{in} = 2.25P_{cr}$; (iii) at a laser power of 320 μJ, the $P_{in} = 4.5P_{cr}$; and (iv) at a laser power of 600 μJ, the $P_{in} = 9.5P_{cr}$, see Figure 3. The relative error bar in the measured experimental data amounts to 8%. Under the investigated conditions, the distribution of a waveguide propagation up to two diffraction lengths (~80 m) without forming a nonlinear focus and plasma column is observed. At higher critical power, $P_{in} > 9.5P_{cr}$, a transverse shape is still close to a Gaussian one. It is seen in Figure 3 that the Gaussian function fit is in good agreement with the measured experimental data. The experiment demonstrates a significant self-phase modulation after measuring with an autocorrelator

https://doi.org/10.1021/acsomega.2c07703
ACS Omega 2023, 8, 3501−3508

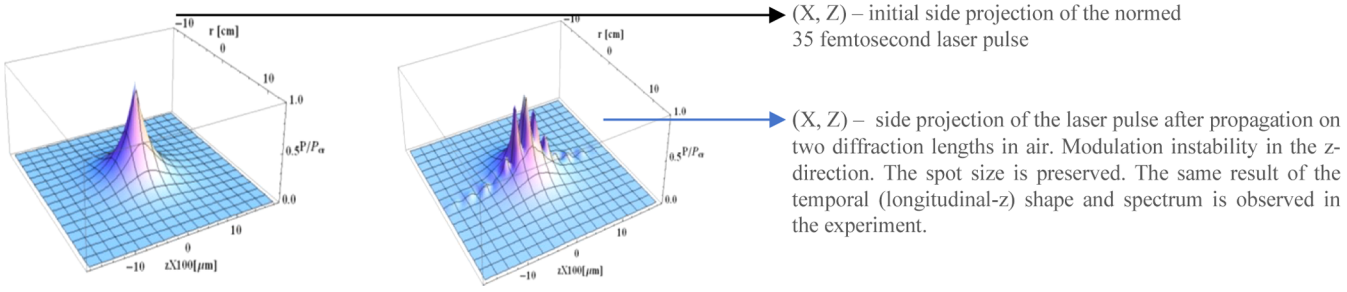

Figure 6. Nonlinear evolution of 35 fs Gaussian pulses pot size of 8 mm and initial power $P_{in} = 9.5P_{cr}$ (600 μJ).

the longitudinal shape of the pulse at 80 m and the initial power $P_{in} > P_{cr.}$ Note here, that at the nanosecond pulse regime, the nonlinear focus appears with a power close to $3P_{cr}$,[19] while in the case of 35 fs pulse, it is observed waveguiding without plasma generation up to $10P_{cr}$,[18] and this is further discussed in the subsection below.

3.1.2. Numerical Investigation. Considering the power region of $1.5P_{cr} < P_{in} < 10P_{cr}$, the nonlinear evolution can be described only by the Kerr type nonlinearity because of the nonlinear addition to the group velocity (self-steepening effect),[20] as well as high order nonlinearity[21] are very small and can be neglected.

This is the reason that the NNAE (2) correctly describes the evolution of the laser pulse with powers slightly above the P_{cr}. The numerical solutions of the NNAE (2) are compared with the well-known spatiotemporal nonlinear equation (STNE), which is obtained after neglecting both nonparaxial terms $\partial^2 A/\partial t_1^2 - \partial^2 A/\partial t_1 \partial z_1$ and then NNAE (2) transforms to STNE:

$$2i\alpha\delta^2\left(\frac{\partial A}{\partial z} + \frac{\partial A}{\partial t}\right) = \Delta_\perp A - \beta\frac{\partial^2 A}{\partial t^2} + \gamma|A|^2 A \quad (3)$$

Under these normalizing conditions, one diffraction length corresponds to $\alpha\delta^2 = 1$. To see the difference between the nano and pico-second nonlinear pulse evolution and this in the femtosecond region, we first solve, numerically, STNE (3) for a nanosecond pulse propagation in air, with initial power $P_{in} > P_{cr}$.

Figure 4 illustrates a typical self-focusing of an optical beam with initial power $P_{in} = 3P_{cr}$, which is sufficient for the formation of a nonlinear focus. The self-focusing with a broad pedestal and the nonlinear focus of the initial Gaussian pulse is obtained at one diffraction length. For higher values of the power, above $P_{in} > 3-10P_{cr}$, the nonlinear focus forms close to the source.[19] In the present experimental findings, we observe a significantly different picture (see Figure 5), where weak self-focusing and wave-guiding up to $P_{in} > 9.5P_{cr}$ are observed. Noticeably, in the femtosecond region, a significantly different regime of nonlinear propagation exists, than the one for the nano- and picosecond pulses. This could be explained due to the light disc's form of the pulse and the role of the nonparaxial terms. Additionally, the nonparaxial terms start to dominate over the transverse Laplacian, responsible for the Fresnel diffraction and the dispersion terms. Therefore, one can expect that NNAE (2) will govern the pulse evolution in the femtosecond region.

Here, we perform numerical simulations by solving NNAE (2) for cases of three different initial laser powers P_{in}, equal to the experimental ones, $1.5P_{cr}$, $2.5P_{cr}$, and $9.5P_{cr}$. It is found, both in the experiment and the numerical simulations, that by increasing P_{in} the self-focusing increases weakly and the laser spot slightly decreases in size. The numerical modeling again confirms the experimental results of waveguiding and weak self-focusing in the case of laser power in the range of $1.5P_{cr} < P_{in} < 10P_{cr}$. The illustration of the compared experimental and numerical results is shown in Figures 3 and 5.

Figure 6 shows the numerical simulation, applying the experimental conditions mentioned above, of the longitudinal deformation of the profile as a result of self-phase modulation. The transverse pulse shape is slightly self-focused, while in the longitudinal direction, several maximums appear as a result of the self-phase modulation.

Summarizing the discussed effects of this regime—the nonlinear waveguiding propagation without ionization, with powers from 1.5 up to 10 times the critical power for self-focusing P_{cr} is discussed. It is demonstrated that compared with the spatiotemporal evolution of nanosecond pulse the nonparaxiality plays a significant role in the femtosecond regime, especially if an initial pulse in a light disc form is performed.

3.2. Single Filamentation. *3.2.1. Experimental Investigation.* In the second discussed regime, a single filament with weak ionization applies, where the laser power is above 10 times the critical power for self-focusing, $P_{in} > 10P_{cr}$. The experimental values for the applied laser power correspond to the range of 600−1200 μJ. Examples of the obtained values are as follows: (i) at a laser power of 800 μJ and corresponding $P_{in} = 12.7P_{cr}$ and (ii) at a laser power of 1000 μJ and the corresponding $P_{in} = 15.5P_{cr}$.

In the performed experiments at a power range of 600−1200 μJ, which is with decades greater than the critical for self-focusing ($P_{in} > 10P_{cr}$), after very weak self-focusing on the center of the pulse spot, starts plasma string formation. Simultaneously with this, the spectra become weakly asymmetric with wings to the short wavelengths. The plasma string from a few centimeters becomes longer by increasing the pulse power. In the initial moment of ionization, the pulse propagation still retains its transverse width, and this propagation regime is known as single filament propagation.[2,3]

Using the fact that the transverse shape does not change significantly, we estimated that the peak intensities are in the order of $10^{10}-10^{11}$ W/cm^2 in the place, where the ionization starts. According to the Eldlich theory for multiphoton ionization, the peak intensities are expected to be at least 10^{13} W/cm^2. The current experimental investigation shows that the ionization starts at 3.5×10^{10} W/cm^2 (laser spot size at 0.8 cm). Increasing the intensity up to 850 μJ, it is found that the laser spot remains while in its center a plasma string is distinguished. Continuing the increase of the intensity up to 850 μJ starts the formation of the plasma beam, and the

https://doi.org/10.1021/acsomega.2c07703
ACS Omega 2023, 8, 3501−3508

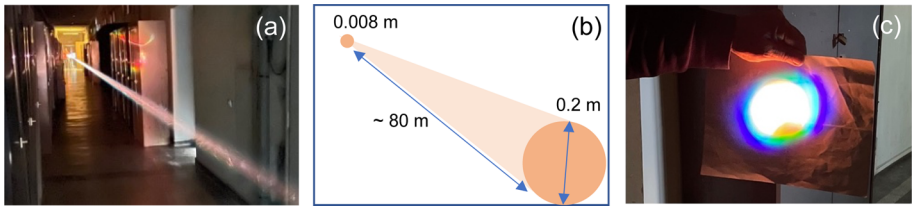

Figure 7. (a) conical beam propagation of the laser beam over 80 m; (b) schematic view of the conical structure of the laser beam with the given dimensions of the beam spot size (0.8 cm from the laser source and 20 cm at ∼50 m); (c) beam shape at 50 m and a spot size of approximately 20 cm.

amplified conical propagation of the laser profile is monitored at laser powers above 1200 μJ.

3.2.2. Theoretical Investigation. The basic studies[3,4] devoted to investigations of the filamentation processes are based on paraxial self-focusing and plasma defocusing, which requests periodical focusing defocusing cycles at a relatively long range of propagation distance. In this investigation, the plasma defocusing starts when the condition $\Delta n = \Delta n_k + \Delta n_i \leq 0$ is fulfilled. Here, $\Delta n_k = n_2 I_0$ is the Kerr-induced nonlinear refractive index, $\Delta n_k = -e^2 N_e / 2\varepsilon_0 m_e \omega_0^2$ is the influence of the plasma generation on the refractive index, N_e is the electron density, e and m are the charge and mass of the electron, respectively, and ω_0 is the carrying frequency of the laser pulse. The defocusing from plasma density overcomes the self-focusing ($\Delta n_i \geq \Delta n_k$) for electron density at least $N_e > 10^{16}$ cm^{-3}. On the other hand, following the formulas of Keldych[22] and Perelomov[23] for multiphoton and tunnel ionization, respectively, it can be seen that this electron density can be achieved at intensities in the order of $I_0 > 1.5 \times 10^{13-14}$ W/cm^2 for infrared (800 nm) pulses. In the present experiments, it is observed that plasma generation starts at intensities of 10^{10} W/cm^2 (850 μJ). With such intensities, as demonstrated by the precise calculations of the ionization rate performed in,[24] there is no optically induced ionization. Based on the experimental and numerical findings, the authors suggest and consider that the stable propagation (single-filament) is simply the nonlinear nonparaxial waveguiding regime discussed above and that the small plasma generation in the center of the pulse (without changing its transverse width) admits quite a different physical origin than the expected multiphoton and tunnel ionization.

3.3. Ionization Instability due to Collision Ionization. To explain the phenomena of the conical emission accompanying the self-guided pulse during filamentation in gasses, several mechanisms and models under different circumstances have been proposed over the last three decades, such as Cherenkov emission and four-photon parametric mixing.[5−7] However, this phenomenon remains still not entirely understood and investigated. The following paragraph proposes a new physical mechanism that could explain the ionization with intensities below 10^{12} W/cm^2 and some of the characteristics of the conical emission by a new type of collision ionization, as suggested in ref 25. Experimentally, it is observed that the conical change-over of the laser pulse profile, starting with a diameter of 0.8 mm at 20 cm from the source, drastically transforms into a colored spot (from deep UV to IR) with a size of approximately 20 cm at a 50 m distance, see Figure 7.

The conical emission is associated with the conical profile of ionization, as it is found in the current experiments. This could also be obtained because of collisional ionization when the ensemble of neutral atoms is initially trapped in the pulse. This ensemble is cooled in the pulse envelope and admits very high kinetic energy due to its translation with the group velocity. The kinetic energy of collision between the cooled trapped particles and the free atoms of the air is of the order of 12−24 GeV, which is high enough to ionize the atoms and molecules. The collision of the trapped and free particles leads to another effect, where the ionized particles are moved in a conical trajectory, as found in the experimental result. As it is known from previous findings in the literature, the multiphoton and tunnel ionization are proportional to the intensity of the laser pulse and appear only in the pulse spots. This is the reason to be suggested here that these types of ionizations cannot generate a conical emission. Therefore, leading us to contemplate a new type of mechanism that could explain this phenomenon. Providing more details regarding the origin of the assumed suggestion, one could start from the longitudinal optical force, which leads to the self-confinement of the neutral air particles into the pulse envelope and their translation with the group velocity. This longitudinal force works in a pulsed regime only and is associated with the Poynting vector and the flow of energy in the direction of propagation. The forces relate to the polarization of atoms and molecules and depend on the initial power, where nonlinear polarization can play a significant role. Furthermore, the longitudinal optical force is inversely proportional to the longitudinal length or temporal duration of the laser pulse, and as a result, the force vanishes in the CW regime, while in the femtosecond region, it leads to the trapping of particles into the pulse envelope. The confinement into the pulse envelope of neutral atoms or molecules (nitrogen's N and oxygen's O_2) in the air can be realized by femtosecond optical pulses. Let us now assume that the trapped pulse envelope particles move along with the group velocity. Then, the kinetic energy of the translation of one nitrogen atom is in the order of 12 GeV, while the energy of the translation of one oxygen molecule is in the order of 24 GeV. The probability of collision with the free atoms and molecules in the air becomes significant if we realize the high density of trapped particles in the pulse's spot. The collision energy in the range of 12−24 GeV is high enough to ionize the atoms after the collision. Consequently, we can expect a new regime of collision ionization when femtosecond pulses propagate in gas. The main differentiation from the well-known multiphoton and tunnel ionization, where all processes are included in the pulse width and depend on intensity, is that the new ionization regime will realize a conical emission of charged particles due to the collisions between trapped particles and free ones. Summarizing, the collision ionization appears at intensities much lower than the ones required for multiphoton and tunnel ionization. The collision ionization by natural means describes the conical emission and the

https://doi.org/10.1021/acsomega.2c07703
ACS Omega 2023, 8, 3501−3508

ionization of the particles with intensities below the ones needed for the photoionization.

4. MAIN FINDINGS AND CONCLUSIONS

Three nonlinear regimes of 35 femtosecond laser pulse propagation in the air are investigated both experimentally and theoretically. Theoretical analyses and numerical simulations are performed to support the experimental results and findings.

A nonlinear waveguide propagation up to two diffraction lengths (~80 m) without forming nonlinear focus and plasma columns is observed under the experimental investigations. The waveguide propagation is detected by preserving the Gaussian profile of the pulse at approximately two diffraction lengths. In the investigated regime 1, the waveguiding propagation without ionization, with laser powers, P_{in} from 1.5 up to 10 times the critical power for self-focusing P_{cr} is discussed. It is demonstrated that, compared with the spatiotemporal evolution of the nanosecond pulse, nonparaxiality plays a significant role in the femtosecond regime, especially if an initial pulse in a light disc form is performed. Increasing the laser power up to $P_{in} = 13P_{cr}$, and reaching regime 2, it is found that the laser spot remains, while in its center, a plasma string is distinguished. By further increase of the laser power up to $P_{in} = 19P_{cr}$ (corresponding to 1200 μJ), thus shifting to regime 3, strong ionization is observed all along the pulse propagation distance and conical emission. A novel mechanism is suggested, based on the longitudinal optical force, which leads to the self-confinement of an ensemble of neutral air particles into the pulse envelope and their translation with the group velocity. This ensemble is cooled in the pulse envelope and admits very high kinetic energy due to its translation with the group velocity. The kinetic energy of collision between the cooled trapped particles and the free atoms of the air is of the order of 12−24 GeV, which is high enough to ionize the atoms and molecules. The collision of the trapped particles and free ones could explain the existence of conical emissions that cannot be described by the known multiphoton and tunnel ionization. The authors believe that the effects described above could be of great interest in the fundamental research areas concerning future in-depth knowledge in the cooling processes, acceleration of neutral particles, and compression of particles by nonlinear mechanisms or by focusing lens,[26] as well as new effects of collision ionization.

AUTHOR INFORMATION

Corresponding Author

Ekaterina Iordanova − *Institute of Solid State Physics, Bulgarian Academy of Sciences, Sofia 1784, Bulgaria;* orcid.org/0000-0002-5767-9021; Email: eiordanova@issp.bas.bg

Authors

Georgi Yankov − *Institute of Solid State Physics, Bulgarian Academy of Sciences, Sofia 1784, Bulgaria*

Stefan Karatodorov − *Institute of Solid State Physics, Bulgarian Academy of Sciences, Sofia 1784, Bulgaria*

Lubomir Kovachev − *Institute of Electronics, Bulgarian Academy of Sciences, Sofia 1784, Bulgaria*

Complete contact information is available at: https://pubs.acs.org/10.1021/acsomega.2c07703

Author Contributions

The manuscript was written primarily through the contributions of E.I. and L.K. Conceptualization, methodology, and investigation were performed by E.I. and L.K. Theoretical and numerical simulations were performed by L.K. Experiments on fs-laser and analyses were performed by G.Y., E.I., and S.K. All authors have approved the final version of the manuscript.

Notes

The authors declare no competing financial interest.

ACKNOWLEDGMENTS

The authors acknowledge the financial support from the BNSF under projects КП-06-ПН58/7-2021 and КП-06-ПН58/8-2021.

ABBREVIATIONS

NNAE, nonlinear nonparaxial amplitude equation; STNE, Spatiotemporal nonlinear equation; CW, continuous wave; GDD, group delay dispersion

REFERENCES

(1) Strickland, D.; Mourou, G. Compression of amplified chirped optical pulses. *Opt. Commun.* **1985**, *56*, 219−221.

(2) Braun, A.; Korn, G.; Liu, X.; Du, D.; Squier, J.; Mourou, G. Self-channeling of high-peak-power femtosecond laser pulses in air. *Opt. Lett.* **1995**, *20*, 73−75.

(3) Couairon, A.; Mysyrowicz, A. Femtosecond filamentation in transparent media. *Phys. Rep.* **2007**, *441*, 47−189.

(4) Chin, S. L.; Hosseini, S. A.; Liu, W.; Luo, Q.; Théberge, F.; Aközbek, N.; Becker, A.; Kandidov, V. P.; Kosareva, O. G.; Schroeder, H. The propagation of powerful femtosecond laser pulses in opticalmedia: physics, applications, and new challenges. *Can. J. Phys.* **2005**, *83*, 863−905.

(5) Skinner, C. H.; Kleiber, P. D. Observation of anomalous conical emission from laser-excited barium vapor. *Phys. Rev. A: At., Mol., Opt. Phys.* **1980**, *21*, 151−156.

(6) Harter, D. J.; Narum, P.; Raymer, M. G.; Boyd, R. W. Four-Wave Parametric Amplification of Rabi Sidebands in Sodium. *Rev. Lett.* **1981**, *46*, 1192.

(7) Golub, I. Optical characteristics of supercontinuum generation. *Opt. Lett.* **1990**, *15*, 305.

(8) Tzortzakis, S.; Méchain, G.; Patalano, G.; André, Y.-B.; Prade, B.; Franco, M.; Mysyrowicz, A.; Munier, J. M.; Gheudin, M.; Beaudin, G.; Encrenaz, P. Coherent subterahertz radiation from femtosecond infrared filaments in air. *Opt. Lett.* **2002**, *27*, 1944−6.

(9) Méchain, G.; Tzortzakis, S.; Prade, B.; Franco, M.; Mysyrowicz, A.; Leriche, B. Calorimetric detection of THz radiation from femtosecond filaments in air. *Appl. Phys. B* **2003**, *77*, 707−709.

(10) Kosareva, O.; et al. Polarization rotation due to femtosecond filamentation in an atomic gas. *Opt. Lett.* **2010**, *35*, 2904−2907.

(11) Tzortzakis, S.; Bergé, L.; Couairon, A.; Franco, M.; Prade, B.; Mysyrowicz, A. Breakup and Fusion of Self-Guided Femtosecond Light Pulses in Air. *Phys. Rev. Lett.* **2001**, *86*, 5470.

(12) Kosareva, O. G.; Panov, N. A.; Akozbek, N.; Kandidov, V. P.; Luo, Q.; Hosseini, S. A.; Liu, W.; Gravel, J.-F.; Roy, G.; Chin, S. L. Controlling a bunch of multiple filaments by means of a beam diameter. *Appl. Phys. B* **2006**, *82*, 111−122.

(13) Shim, B.; Schrauth, S. E.; Hensley, C. J.; Vuong, L. T.; Hui, P.; Ishaaya, A. A.; Gaeta, A. L. Controlled interactions of femtosecond light filaments in air. *Phys. Rev. A: At., Mol., Opt. Phys.* **2010**, *81*, 061803.

(14) Kovachev, L. M.; Dakova, D. A.; Dakova, A. M. Influence of the four-photon parametric processes and cross-phase modulation on the relative motion of optical filaments. *Laser Phys.* **2015**, *25*, 105402.

(15) Méchain, G.; Couairon, A.; André, Y.-B.; D'Amico, C.; Franco, M.; Prade, B.; Tzortzakis, S.; Mysyrowicz, A.; Sauerbrey, R. Long-

range self-channeling of infrared laser pulses in air: a new regime without ionization. *Appl. Phys. B* **2004**, *79*, 379−382.
(16) Dubietis, A.; Gaižauskas, E.; Tamošauskas, G.; Di Trapani, P. Light filaments without self-channeling. *Phys. Rev. Lett.* **2004**, *92*, 253903.
(17) Kovachev, M. Collapse arrest and self-guiding of femtosecond pulses. *Opt. Express* **2007**, *15*, 10318−23.
(18) Iordanova, E.; Yankov, G.; Karatodorov, S.; Kovachev, L.Linear and nonlinear waveguiding of femtosecond pulses in air; *COFIL-2022 Conference*; Book of Abstracts, 2022; pp 121−122.
(19) Marburger, J. H. Self-focusing: Theory. *Progr. Quant. Elect.* **1975**, *4*, 35−110.
(20) Rothenberg, J. E. Space-time focusing: breakdown of the slowly varying envelope approximation in the self-focusing of femtosecond pulses. *Opt. Lett.* **1992**, *17*, 1340−1342.
(21) Petrarca, M.; Petit, Y.; Henin, S.; Delagrange, R.; Bejot, P.; Kasparian, J. Higher-order Kerr improve quantitative modeling of laser filamentation. *Opt. Lett.* **2012**, *37*, 4347.
(22) Keldysh, L. V. Ionization in the field of a strong electromagnetic wave. *Sov. Phys.—JETP* **1965**, *20*, 1307−1314.
(23) Perelomov, A. M.; Popov, V. S.; Terent'ev, M. V. Ionization of atoms in an alternating electric field. *Sov. Phys.—JETP* **1966**, *23*, 924−934.
(24) Couairon, A.Mysyrowicz, AFemtosecond Filamentation in Air. In *Progress in Ultrafast Intense Laser Science Volume I. Springer Series in Chemical Physics*; Springer: Berlin, Heidelberg, 2006; Vol. *84*.
(25) Kovachev, L. M. Radiation forces and confinement of neutral particles into the pulse envelope. New regime of collision ionization. *Optik* **2022**, *269*, 169943.
(26) Yankov, G.; Iordanova, E.; Kovachev, L. M. "Radiation forces and compression of neutral particles by an optical lens". *Optik* **2023**, *273*, 170452.

https://doi.org/10.1021/acsomega.2c07703
ACS Omega 2023, 8, 3501−3508